

An efficient computational method for stress concentration problems

Santosh Shrestha[†] and Mitao Ohga[‡]

*Department of Civil and Environmental Engineering, Ehime University,
3, Bunkyo-Cho, Matsuyama 790-8577, Japan*

(Received July 5, 2005, Accepted December 9, 2005)

Abstract. In this paper a recently developed scaled boundary finite element method (SBFEM) is applied to simulate stress concentration for two-dimensional structures. In addition, a simple and independent formulation for evaluating the coefficients, not only of the singular term but also higher order non-singular terms, of the stress fields near crack-tip is presented. The formulation is formed by comparing the displacement along the radial points ahead of the crack-tip with that of standard Williams' eigenfunction solution for the crack-tip. The validity of the formulation is examined by numerical examples with different geometries for a range of crack sizes. The results show good agreement with available solutions in literatures. Based on the results of the study, it is conformed that the proposed numerical method can be applied to simulate stress concentrations in both cracked and uncracked structure components more easily with relatively coarse and simple model than other computational methods.

Keywords: stress concentration; scaled boundary finite element method; stress intensity factor; T -stress; higher order terms.

1. Introduction

Failure of a structure is often a result of a complex process of crack initiation, growth and fracture pattern formation. Because of this, the failure prediction can be divided into two different methods. The first method examines the stress concentrations at notches, corners, holes etc. of uncracked engineering components because cracks are likely to initiate at that region under the action of fatigue loading due to the stress concentration. The second method examines the stress concentration near a crack-tip of the cracked structure components using fracture mechanics because the stress and displacement fields near a crack-tip govern fracture process that takes place at the crack-tip. In both of these methods, understanding and accurate modeling of the stress concentrations in conjunction with a crack growth condition are vital to implement simulation essential for failure prediction due to the fact that most structure components fail from the stress concentration.

The finite element method (FEM) and the boundary element method (BEM) are most widely used computational methods to perform numerical simulation for failure prediction. Although the

[†] Graduate Student

[‡] Professor, Corresponding author, E-mail: ohga@dpc.ehime-u.ac.jp

traditional FEM is very versatile, the method has some serious limitations in solving certain problems: stress concentration and crack propagation. For such problems, the use of FEM requires a large number of discretization which reduces its efficiency. On the other hand, the BEM has certain advantages over the domain type method, like FEM, because it only needs boundary discretization of the studied problems. But BEM needs a lot of mathematical skills because in numerical implementation, one needs fundamental solution, which is not always available, or it can be very complicated even if it exists, and also needs an advanced mathematical knowledge to deal with various singular integrals. Besides, the standard FEM and BEM are based on assumed piecewise smooth functions, which do not resemble the exact solution near the singular point (Oh and Babuska 1992).

In this paper, a recently developed computational method called scaled boundary finite element method (SBFEM), which is emerging as an alternative approach in order to overcome the deficiencies of FEM and BEM, is proposed as an efficient and comparatively accurate numerical method for modeling stress concentrations of failure components. The method has some unique properties that provide distinct advantages for its application in stress concentration and crack problem. The main advantages of SBFEM over the traditional methods are that analytical solutions are obtained in one dimension without fundamental solution, and removes the necessity to discretize certain free and fixed boundaries when the so called 'scaling center' lies on the interested point. In addition, SBFEM is mathematically simple and straightforward, making it a versatile tool compared to conventional BEM although it requires eigenvalue solution in its implementation. As will be discussed later, SBFEM has a unique capacity to more accurately compute stress and displacement field of singularities region at the interested region without any *a priori* assumption.

Since SBFEM is a new method, its application has not been fully explored in many fields of engineering mechanics, especially in the stress concentration and fracture problems. In these regards, Deeks and Wolf (2002a-c) have demonstrated that the SBFEM out-performs the FEM in situations involving stress concentrations or unbounded domains, reducing significantly the program run-time for the same accuracy. Song and Wolf (2002), Deeks (2002) have applied SBFEM to determine stress intensity factors (SIFs) in two-dimensional problems. Recently, Song (2004) applied SBFEM to determine dynamic SIFs by using super elements. In addition, in the linear elastic fracture mechanics, recent studies show that not only a single parameter – SIFs but also other parameters - constant (*T*-stress) and higher order non-singular terms of stress field are of great relevance in characterizing the fracture behaviors (Du and Hancock 1991, Dyskin 1997, Jeon and Im 2001, Karihaloo and Xiao 2001, Larsson and Carlsson 1973, Yang *et al.* 1993); and the determination of these coefficients has drawn significant attention over the last few years (Karihaloo and Xiao 2001).

Thus, the main purpose of this paper is to demonstrate the efficiency and effectiveness of the method to model the stress concentration; and also to extend the application of SBFEM for computing more than one fracture parameters for two-dimensional linear-elastic cracked structures. To compute the fracture parameters, a simple and direct technique is presented by comparing the displacement along the radial points ahead of the crack-tip with that of standard Williams' eigenfunction expansion of the linear elastic displacement field at the crack-tip. The technique presented in this paper can be applied directly as well as independently to evaluate coefficients of the stress fields and has more advantages than other methods because of its simplicity in expression and less computational efforts in implementation. Recently, Song (2005), Chidgzy and Deeks (2005) have also applied SBFEM to compute these coefficients.

2. Scaled boundary finite element method

The scaled boundary finite element method is a semi-analytical fundamental solution-less BEM based on FEM (Wolf 2003). It is semi-analytical in the sense that it transforms the partial differential equation of a variety of linear problems into ordinary differential equations. These ordinary differential equations are solved analytically in radial direction and the coefficients of these equations are determined by the finite element approximation in the circumferential directions. The virtual work derivations of the stress and displacement fields in the method are presented in detail in Deeks and Wolf (2002c) but are summarized here for convenience as follows.

2.1 Governing equations of elastostatics

For two-dimensional elastostatic problems, the strains $\{\varepsilon(x, y)\}$ are related to the displacement $\{u(x, y)\}$ by

$$\{\varepsilon(x, y)\} = \begin{Bmatrix} \varepsilon_x \\ \varepsilon_y \\ \gamma_{xy} \end{Bmatrix} = \begin{Bmatrix} \partial/\partial x & 0 \\ 0 & \partial/\partial y \\ \partial/\partial y & \partial/\partial x \end{Bmatrix} \begin{Bmatrix} u_x \\ u_y \end{Bmatrix} = [L]\{u(x, y)\} \quad (1)$$

where, $[L]$ is linear differential operator, and the stresses $\{\sigma(x, y)\} = [\sigma_x, \sigma_y, \tau_{xy}]^T$ are given by

$$\{\sigma(x, y)\} = \{\varepsilon(x, y)\} = [D][L]\{u(x, y)\} \quad (2)$$

In no body load case, the internal equilibrium in elastostatics leads to the differential equation

$$[L]^T\{\sigma(x, y)\} = 0 \quad (3)$$

which must be satisfied at every point within the domain.

2.2 Scaled boundary coordinate system

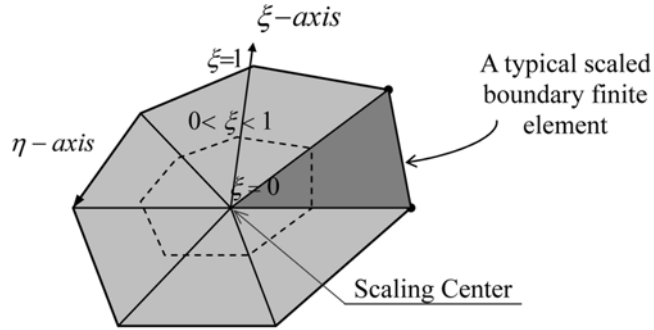
The SBFEM coordinate system consists of a radial direction ξ and a local circumferential direction η (Fig. 1). The radial coordinate is defined to be zero at 'scaling center', and have unit value on the boundary. The circumferential coordinate measures the distance anticlockwise around the boundary. The coordinate system is termed the scaled boundary coordinate system, and is related to Cartesian coordinate by

$$x = x_0 + \xi x(\eta) \quad (4a)$$

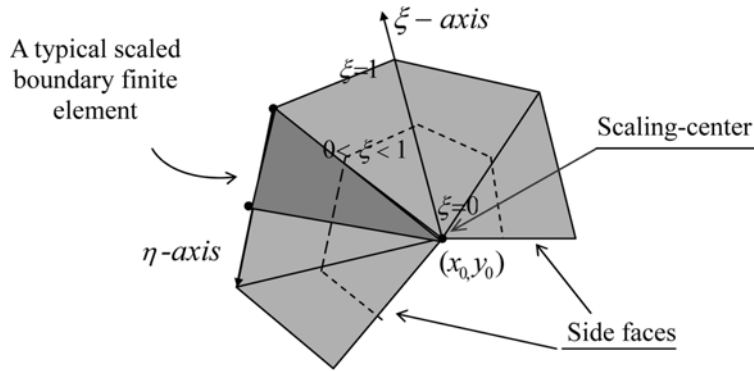
$$y = y_0 + \xi y(\eta) \quad (4b)$$

where, $x(\eta)$ and $y(\eta)$ are the functions describing the variation of the boundary in x and y directions as functions of η .

Applying standard procedures to transform the geometry from Cartesian co-ordinates to the scaled



(a) Closed boundary



(b) Open boundary

Fig. 1 Scaled boundary coordinate system

boundary co-ordinates defined in Eq. (4), the linear operator in Eq. (3) can be written in the coordinate ξ, η as

$$[L] = [b^1(\eta)] \frac{\partial}{\partial \xi} + \frac{1}{\xi} [b^2(\eta)] \frac{\partial}{\partial \eta} \tag{5}$$

where, $[b^1(\eta)]$ and $[b^2(\eta)]$ depend only on the geometry of the boundary.

2.3 Displacement function

The displacements at any point in the domain defined by scaled boundary coordinates (ξ, η) can be expressed in the form:

$$\{u(\xi, \eta)\} = \sum_{i=1}^n N_i(\eta) \{u_i(\xi)\} = [N(\eta)] \{u(\xi)\} \tag{6}$$

which represents a discretization of boundary only.

Substituting Eqs. (5) and (6) in Eq. (2) leads to the approximate stresses in the co-ordinate ξ, η as

$$\{\sigma(\xi, \eta)\} = [D][B^1(\eta)]\{u(\xi)\}_{,\xi} + \frac{1}{\xi}[D][B^2(\eta)]\{u(\xi)\} \quad (7)$$

where,

$$[B^1(\eta)] = [b^1(\eta)][N(\eta)] \quad (8a)$$

$$[B^2(\eta)] = [b^2(\eta)][N(\eta)]_{,\eta} \quad (8b)$$

These results can be used in the virtual work equation to solve for the radial displacements.

2.4 Scaled boundary finite element equation

The virtual work statement is applied to introduce the equilibrium. When the domain is subjected to a set of boundary tractions $\{t\}$, the virtual work statement is

$$\int_V \{\delta\varepsilon\}^T \{\sigma\} dV = \int_S \{\delta u\}^T \{t\} ds \quad (9)$$

Performing integrals over the domain and then a series of mathematical manipulations, the virtual work statement is satisfied for all virtual displacements $\{\delta u(\xi)\}$ when

$$[E^0]\xi^2\{u(\xi)\}_{,\xi\xi} + [[E^0] + [E^1]^T - [E^1]]\xi\{u(\xi)\}_{,\xi} - [E^2]\{u(\xi)\} = 0 \quad (10)$$

where, the coefficient matrices

$$[E^0] = \int_{-1}^1 [B^1]^T [D] [B^1] |J| d\eta \quad (11a)$$

$$[E^1] = \int_{-1}^1 [B^2]^T [D] [B^1] |J| d\eta \quad (11b)$$

$$[E^2] = \int_{-1}^1 [B^2]^T [D] [B^2] |J| d\eta \quad (11c)$$

are independent of ξ . Eq. (10) is a standard ordinary differential equation for the displacements $u(\xi)$ with the dimensionless radial coordinate ξ as the independent variable.

2.5 Solution procedures

By inspection, solution to the set of Euler-Cauchy differential equation represented by Eq. (10) must be of the form

$$\{u(\xi)\} = \sum_{i=1}^n c_i \xi^{-\lambda_i} \{\phi_i\} \quad (12)$$

where, the exponents λ_i and vectors $\{\phi_i\}$ are interpreted as a radial scaling factor and a displacement mode shapes, respectively. Substituting this solution into Eq. (10) yields the quadratic eigenproblem.

$$[\lambda^2[E^0] - \lambda[[E^1]^T - [E^1]] - [E^2]]\{\phi\} = 0 \quad (13)$$

This eigenproblem can be solved using standard techniques, yielding $2n$ displacement modes, where n is the number of nodes used in boundary discretization, and hence is also the size of the coefficient matrices.

Bounded problems can be represented conveniently by taking $0 \leq \xi \leq 1$. For such problems, only n modes with negative real component of λ lead to finite displacements at scaling center. This subset of n nodes is denoted by $[\Phi_1]$. For any set of boundary node displacements, u , the integration constants are

$$\{c\} = [\Phi_1]^{-1}\{u\} \quad (14)$$

The displacement fields can be obtained using

$$\{u(\xi, \eta)\} = [N(\eta)] \sum_{i=1}^n c_i \xi^{-\lambda_i} \{\phi_i\} \quad (15)$$

and the stress field is

$$\{\sigma(\xi, \eta)\} = [D] \sum_{i=1}^n [c_i \xi^{-\lambda_i-1} [-\lambda_i [B^1(\eta)] + [B^2(\eta)]] \{\phi_i\}] \quad (16)$$

Eqs. (15) and (16) are the semi-analytical solutions for displacement and stress fields inside the domain, respectively.

3. SBFEM formulation for fracture parameters

Williams' eigenfunction expansion (Williams 1957) for crack-tip displacement field in any linear elastic body is given by a series of the form

$$\begin{aligned} \begin{Bmatrix} u_1 \\ u_2 \end{Bmatrix} &= \frac{K_I}{4G} \left(\frac{r}{2\pi}\right)^{1/2} \begin{Bmatrix} (2\kappa-1)\cos\left(\frac{\theta}{2}\right) - \cos\left(\frac{\theta}{2}\right) \\ (2\kappa+1)\sin\left(\frac{\theta}{2}\right) - \sin\left(\frac{\theta}{2}\right) \end{Bmatrix} + \frac{Tr}{2G} \begin{Bmatrix} (\kappa+1)\cos\theta \\ (\kappa-2)\sin\theta \end{Bmatrix} \\ &+ \sum_{n=3}^{\infty} \frac{r^{n/2}}{2G} a_n \begin{Bmatrix} \left(\kappa + \frac{n}{2} + (-1)^n\right)\cos\left(\frac{n}{2}\right)\theta - \frac{n}{2}\cos\left(\frac{n}{2}-2\right)\theta \\ \left(\kappa - \frac{n}{2} - (-1)^n\right)\sin\left(\frac{n}{2}\right)\theta + \frac{n}{2}\sin\left(\frac{n}{2}-2\right)\theta \end{Bmatrix} \end{aligned} \quad (17)$$

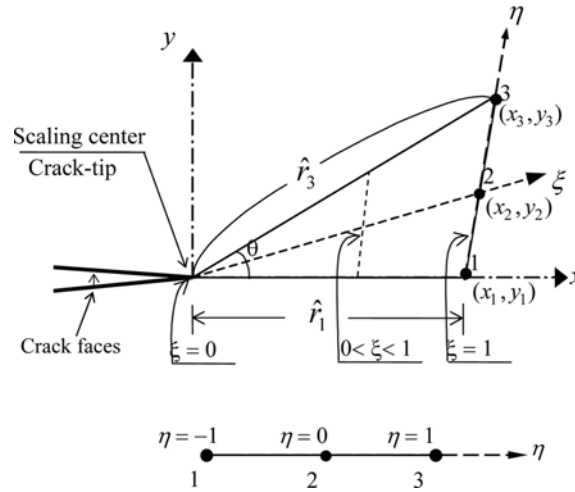


Fig. 2 A typical SBFEM element in a crack analysis

where (r, θ) are the local polar coordinates with the origin at the crack-tip, as shown in Fig. 2; $\mu = E/(2(1 + \nu))$ is the shear modulus; the Kolosov constant $\kappa = 3 - 4\nu$ for plane strain or $\kappa = (3 - \nu)/(1 + \nu)$ for plane stress; E and ν are Young's modulus and Poisson's ratio, respectively. K_I is the SIF for mode I , T is the elastic T -stress, and A_n is the higher order coefficient term. The first term consisting of the singular component is referred to as the singular term and the remaining terms regular in the radial co-ordinate r are referred to as the non-singular terms.

In SBFEM analysis, the stress and displacement fields along the radial direction emanating from the crack tip can be analytically calculated when the so-called 'scaling center' is chosen at a crack-tip, as shown in Fig. 2. Only the boundaries, but not the straight crack faces and faces passing through the crack-tip are discretized.

The SBFEM's displacement field inside the domain of Eq. (15) can be expanded as

$$\begin{aligned}
 u(\xi, \eta) &= U_1 \xi^{1/2} + U_2 \xi + U_3 \xi^{3/2} + \dots + A_n \xi^{n/2} \\
 &= \sum_{i=1}^n U_i \xi^{i/2}
 \end{aligned}
 \tag{18}$$

where the coefficients

$$U_i = c_i \{ \phi \}_i
 \tag{19}$$

and the power terms

$$\lambda_i = -\frac{i}{2} \quad \forall \quad i = 1, 2, 3, \dots, n
 \tag{20}$$

For a radial direction emanating from the crack tip and inclined at an angle θ to the global x -axis as shown in Fig. 2, the following relationships are obtained from Eq. (4).

$$r = r(\xi, \eta) = \xi \hat{r}
 \tag{21}$$

and
$$\tan \theta = \frac{y(\eta)}{x(\eta)} \quad (22)$$

where, $\hat{r} = r(\eta) = \{x(\eta)^2 + y(\eta)^2\}^{1/2}$ is the radial distance of the boundary nodes from scaling center, and r is a distance measured from the crack-tip along the radial lines. The angle θ and the distance \hat{r} are constants for a given radial line of a given element.

Substituting Eq. (21), Eq. (18) becomes

$$u(\xi, \eta) = \sum_{i=1}^n U_i \hat{r}^{-i/2} r^{i/2} \quad (23)$$

Eq. (23) is similar to the Williams' expansion of the displacement field, Eq. (17). Thus, the stress intensity factors, T -stress, and higher order coefficient terms of stress field near crack-tip can be computed by equating the coefficients of like powers of r terms of Eqs. (23) and (17). The proposed formulations of fracture parameters for $\theta = 0$ are as follows.

Stress intensity factor for mode I ,

$$K_I = \frac{2G}{\kappa - 1} U_1 \sqrt{\frac{2\pi}{\hat{r}}} \quad (24)$$

T -stress,

$$T = \frac{2G}{\kappa + 1} \left(\frac{U_2}{\hat{r}} \right) \quad (25)$$

and higher coefficients terms,

$$a_n = \frac{2G}{\kappa + (-1)^n} U_n \hat{r}^{-n/2} \quad \forall n = 3, 4, 5, \dots \quad (26)$$

Eqs. (24), (25) and (26) indicate that the SIFs, T -stress of the Williams' series can be directly calculated from SBFEM.

4. Numerical examples

In this section, the following three numerical examples for two-dimensional stress concentration problems are simulated to demonstrate the effectiveness of the SBFEM, and additionally to verify the validity of the proposed SBFEM formulation of fracture parameters.

- (i) Square holed compression plate
- (ii) Central crack rectangular plate, and
- (iii) A T -joint weld attachment with a horizontal crack in the main plate

In order to demonstrate the effectiveness of the proposed SBFEM, the results obtained by using this method are compared with the corresponding results of FEM; and the validity of the proposed formulation is checked by comparing the results of the method with analytical and numerical results from literatures. In all of the example problems, the discretizations employed in the study consist of three-noded line elements in SBFEM analyses and a combination of four-noded quadratic elements and three-noded triangular elements are used in FEM analyses.

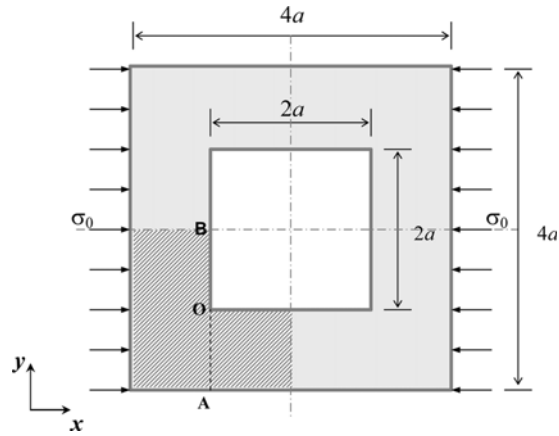


Fig. 3 Schematic diagram of square-holed compression plate

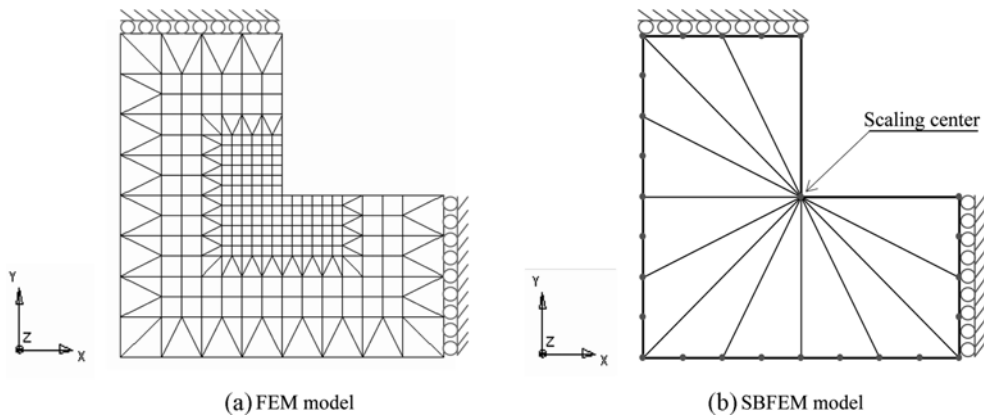


Fig. 4 Discretization models for square-holed compression plate

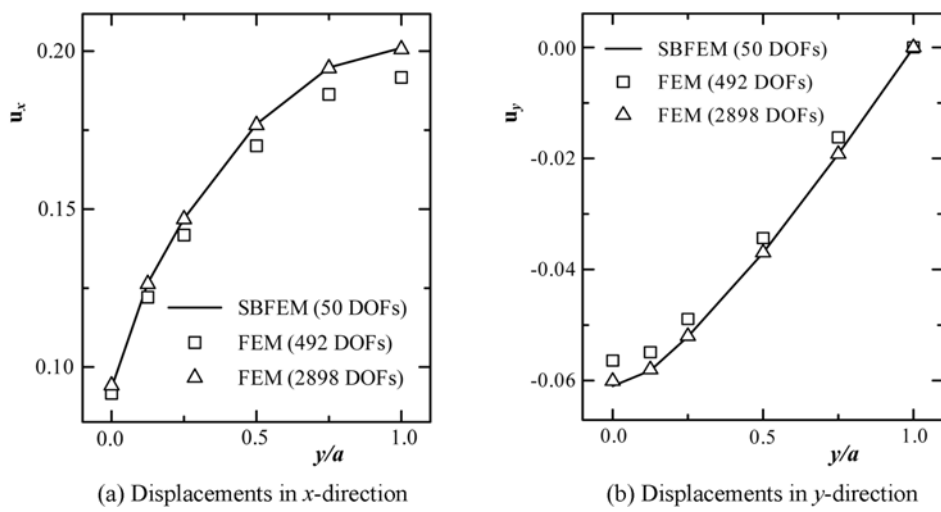


Fig. 5 Comparison of displacements along OB

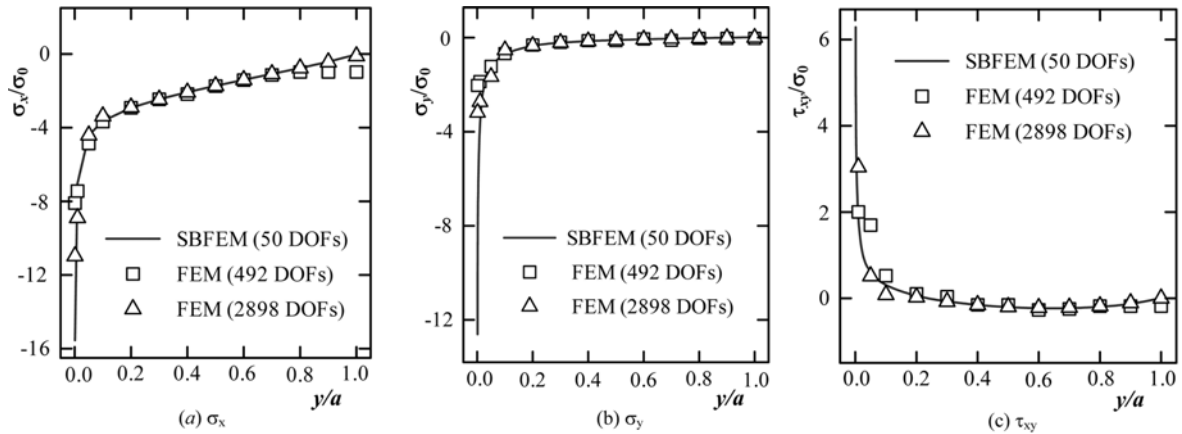


Fig. 6 Comparison of stress components along OA

4.1 Example 1: Square-holed compression plate

The first example is a square-holed rectangular plate with uniaxial compression, as shown in Fig. 3. The objective is to predict the stresses near the sharp corner where the stress singularity exists and the displacements along inner face by using SBFEM and to verify the effectiveness of SBFEM by comparing with corresponding FEM results. The analyses were carried out using plane stress condition. The modulus of elasticity (Young's modulus) E was 1.0 and Poisson's ratio ν was 0.25. The applied stress σ_0 was equal to 1 with its units consistent with that of E . A unit thickness of plate was assumed. Due to the biaxial symmetry, only one quadrant, i.e., the hatched portion in Fig. 3, was modeled using one SBFEM and two FEM discretizations. The FEM mesh with 246 nodes (492 DOFs) and SBFEM mesh with 25 nodes (50 DOFs) are illustrated in Figs. 4(a) and (b), respectively. Since there are stress singularities at the internal corners, the scaling center was placed at the corner and the inner faces were not discretized in SBFEM analysis as shown in Fig. 4(b). Only the symmetric faces and the exterior boundary surfaces were discretized. In the FEM analysis, the mesh near the internal corner was refined as compared with other parts, as shown in Fig. 4(a).

The computed displacements along OB (Fig. 3) of SBFEM are presented in Fig. 5 with those of FEM with 492 and 2868 DOFs. This comparative graphs clearly show that the SBFEM results with less than 2 percentage DOFs are significantly similar to that of the fine mesh FEM. Fig. 6 presents the comparison of stress components (σ_x , σ_y and τ_{xy}) along OA (Fig. 3) computed by FEM with 492 and 2868 DOFs and SBFEM with 50 DOFs. The comparison shows that SBFEM results are in good agreement with FEM results except near the singularity region i.e., near the inner corner. In the singularity region, FEM results increase with increase in DOFs, but the SBFEM results are higher values than the fine mesh FEM results near the corner with much less number of DOFs. Fig. 7 shows the contour of stress in x -direction (σ_x).

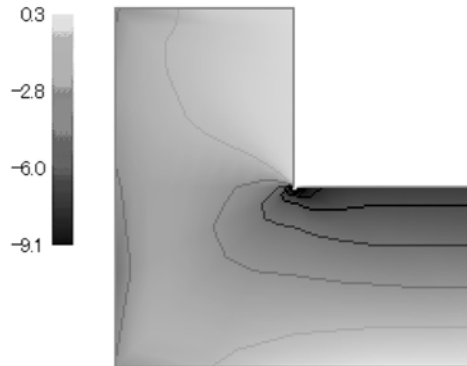


Fig. 7 Contour of stress in x -direction (σ_x)

4.2 Example 2: Central-cracked rectangular plate

The second problem consists of a center-cracked rectangular plate with uniaxial tension. The schematic diagram of the problem is presented in Fig. 8, where H and W are plate dimensions and a is the crack length. In this problem, the stress along y -axis σ_y ahead of the crack-tip and the coefficients, a_n ($1 \leq n \leq 10$), of the asymptotic fields near the crack-tip were evaluated by using Eq. (16) and the proposed SBFEM formulations (Eqs. (24) to (26)), respectively. The objective of first analysis i.e., computation of near tip stress is to demonstrate efficiency of SBFEM compared to FEM, and that of the second analysis is to verify the validity of the proposed formulation.

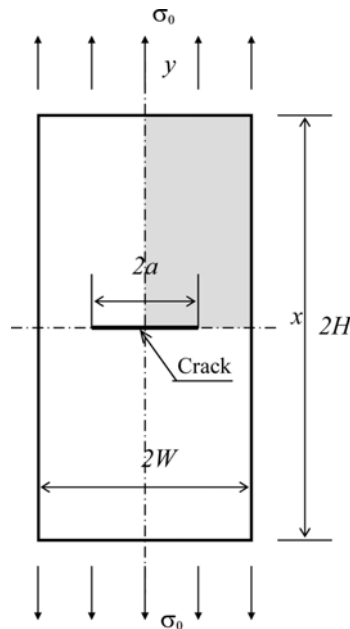


Fig. 8 Schematic diagram of central cracked rectangular plate under uniaxial tension

The analyses were carried out using plane stress condition with Young's modulus $E = 1.0$ and Poisson's ratio $\nu = 0.3$. The applied stress was $\sigma_0 = 1$ with its units consistent with that of E . A unit thickness of plate was assumed. The problem is a biaxial and symmetric, and therefore only one quadrant (highlighted portion in Fig. 8) was modeled. The FEM and SBFEM analysis models are shown in Fig. 9. Note that the scaling center i.e., plus sign in the Fig. 9(c), was placed at the crack-tip in SBFEM mesh. Crack face, which was assumed as a straight face, and face through the crack-

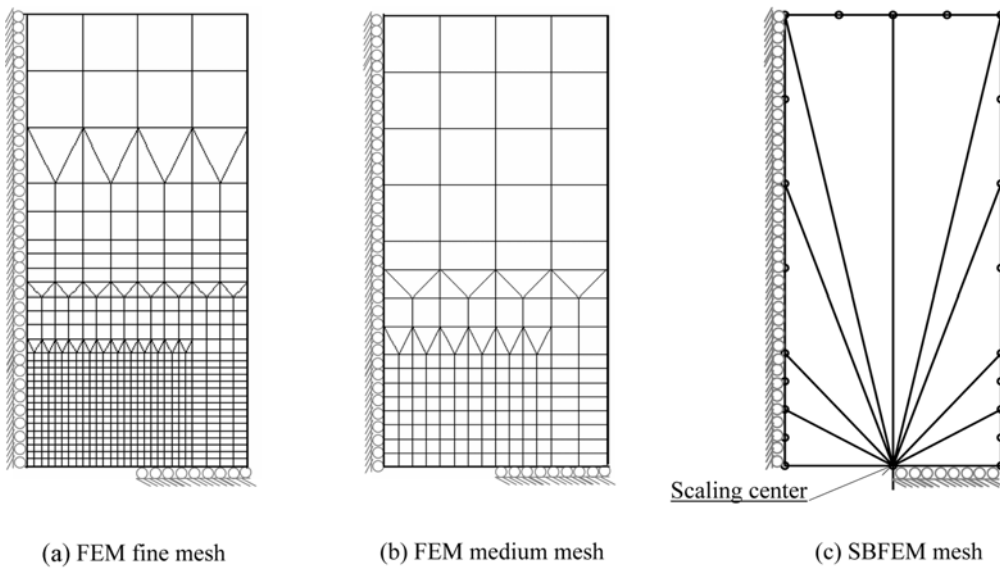


Fig. 9 Discretization models of central cracked rectangular plate

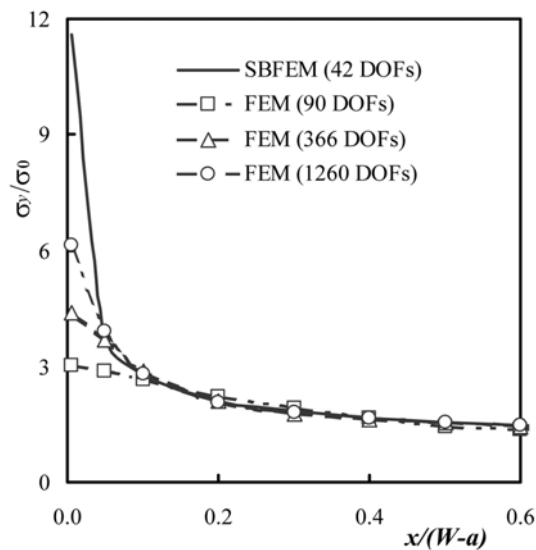


Fig. 10 Comparison of stress ahead of the crack-tip in y -direction (σ_y)

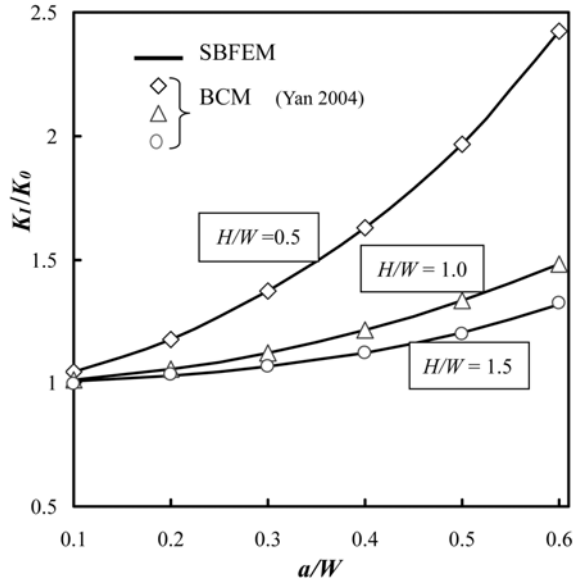


Fig. 11 Comparison of normalized SIFs

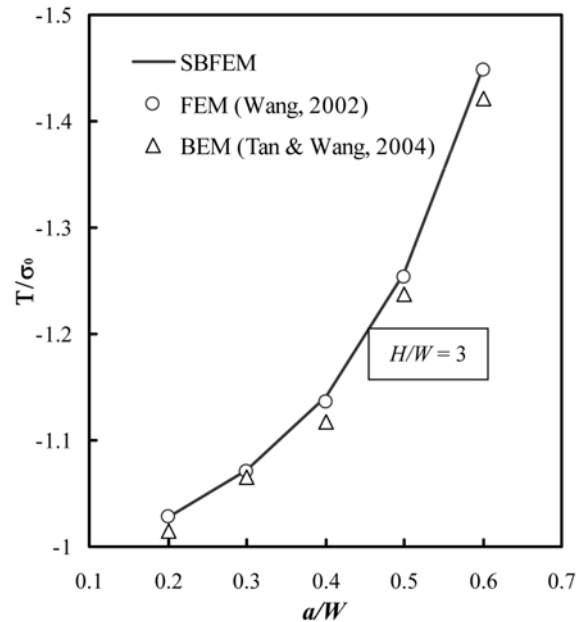


Fig. 12 Comparison of normalized T -stress

tip were not discretized. The SBFEM analysis was performed with single discretization of 42 DOFs and the FEM analysis was performed with three different discretizations – coarse of 90 DOFs, medium of 366 DOFs and fine of 1260 DOFs. The FEM medium and fine meshes are shown in Figs. 9(a) and (b), respectively. Fig. 10 presents the plots of computed stress σ_y , normalized by applied stress σ_0 , σ_y/σ_0 , of a SBFEM and three FEM analyses as a function of $x/(W - a)$. As in first example, the Fig. 10 shows close agreement of all the computed results, except in the region near crack-tip, where singularity occurs. In the singularity region, singularity of FEM results increase with increase in number of nodes, but SBFEM results show more singularity than fine mesh FEM results.

To compute the SIFs, T -stress and non-singular higher order terms, and to verify the validity of the proposed SBFEM technique, analysis was carried out for a range of geometrical configurations with variety of crack sizes. The computed results of normalized SIFs, K_I/K_0 , where $K_0 = \sigma_0(\pi a)^{1/2}$, for $H/W = 0.5, 1$ and 1.5 and normalized T -stress, T/σ_0 , for $H/W = 3$ were compared with the values of boundary collocation method (BCM) presented in Yan (2004) and the values of FEM and BEM from Wang (2002) and Tan and Wang (2003) in Figs. 11 and 12, respectively. In Table 1, the first–fifth coefficients terms of the stress field near the crack-tip for $a = 1, W = H = 4$ are compared with the results of hybrid crack element (HCE) and BEM from Xiao *et al.* (2004). These comparisons show that SBFEM results are generally in good agreement with the literature values. The coefficients of sixth to tenth terms of the stress fields which, to the authors’ knowledge, have not been done before are also presented in the Table 1.

Table 1 Coefficients, a_n ($1 \leq n \leq 10$) in Eq. (28), of the stress field near the crack-tip

Terms	Coefficients			Ratio*	
	Present	Xiao <i>et al.</i> (2004)		BCM	HCE
a_i	SBFEM	BCM	HCE	BCM	HCE
a_1	0.7675	0.7680	0.7665	0.9993	1.0013
a_2	-0.2774	-0.2777	-0.2779	0.9989	0.9982
a_3	0.1865	0.1866	0.1915	0.9995	0.9739
a_4	0.0030	0.0030	0.0018	1.0000	1.6667
a_5	-0.0278	-0.0279	-0.0235	0.9964	1.1830
a_6	0.0008	-	-	-	-
a_7	0.0057	-	-	-	-
a_8	-0.0001	-	-	-	-
a_9	-0.0018	-	-	-	-
a_{10}	0.00001	-	-	-	-

*Ratio = computed SBFEM value/reference value

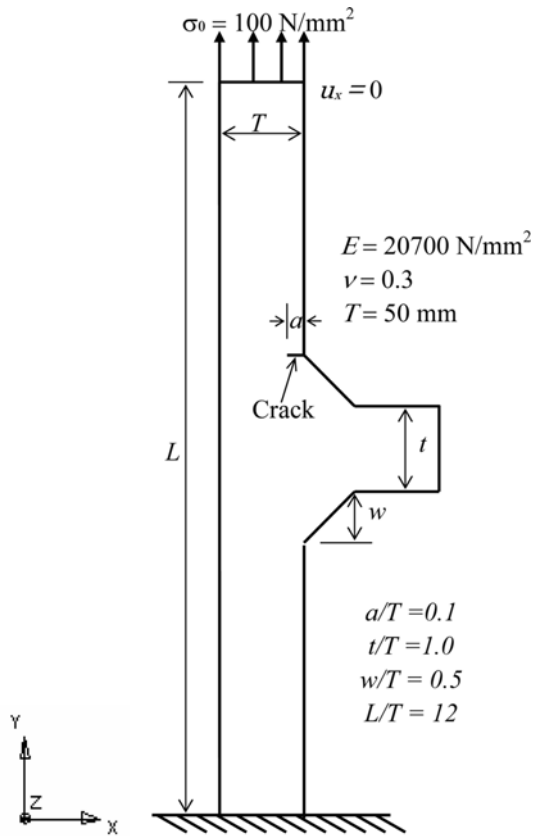


Fig. 13 Schematic diagram of T-joint weld attachment with a horizontal crack in the main plate under uniform tension

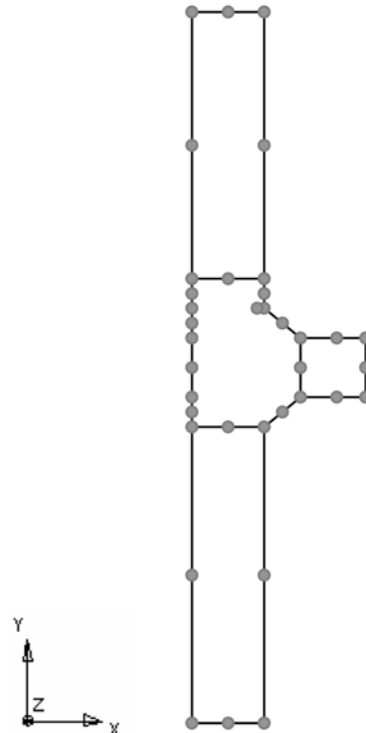


Fig. 14 A SBFEM discretization model of T-joint weld plate attachment with a horizontal crack in the main plate

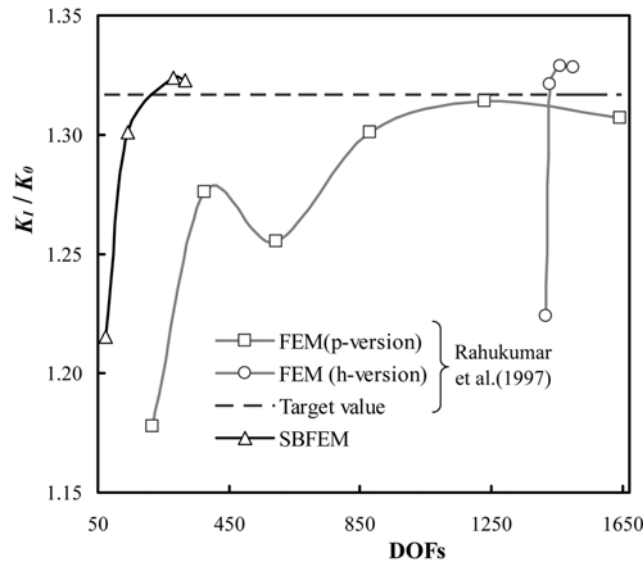


Fig. 15 Comparison of computed normalized SIFs

4.3 Example 3: A T-joint weld attachment with a horizontal crack in the main plate

In this problem, the SBFEM formulation is applied to more complex crack problems to compute SIFs. The problem has some significance in engineering practices. A T-joint weld unit thickness attachment with a horizontal crack in the main plate and a uniaxial tension of $\sigma_0 = 100 \text{ N/mm}^2$ applied to the main plate, as shown in Fig. 13, was considered. Plane stress conditions were assumed. The material properties employed were $E = 20700 \text{ N/mm}^2$ and $\nu = 0.3$. The other parameters used for the analysis are presented in Fig. 13. The top edge of the plate, where the external load is applied, was restrained from displacement in x -direction.

The SBFEM analysis for this configuration was performed using sub-structuring as shown in mesh diagram (Fig. 14). One of the restrictions of SBFEM is that the entire boundary must be visible from the scaling center. So the model was divided into four sub-domains for SBFEM analysis. The computed SBFEM results of the normalized SIFs from four different refined meshes are compared with the FEM (p -version and h -version) results from Rahukumar *et al.* (1997) in Fig. 15. The target values of the normalized SIFs, K_I/K_0 , where $K_0 = \sigma_0(\pi a)^{1/2}$, is also taken from Rahukumar *et al.* (1997). The figure clearly shows that the SBFEM results are in good agreement with the results of p -version and h -version FEM and converges rapidly with much less DOFs. In addition SBFEM does not require discretization of crack faces or region near the crack-tip. Hence no special care is needed, like in p -version FEM, in the design of meshes for SBFEM analysis.

5. Conclusions

The scaled boundary finite element method (SBFEM) has been applied to simulate two-dimensional linear elastic stress concentration problems. The accuracy and efficiency of the SBFEM

has been examined by comparing the computed SBFEM results with that of FEM. The SBFEM outperformed the FEM regarding efficiently in terms of number of degrees of freedoms and qualitatively accurate result in stress concentration region; this result is in agreement with the results of the previous studies. In addition, a simple and direct formulation has been derived for evaluating more than one fracture parameters of a cracked body by comparing the classical linear elastic field solution in the vicinity of a crack-tip to that of SBFEM after power series expansion. The validity of these formulations has been examined with two example problems for a range of crack sizes, with good agreement obtained between the SBFEM results obtained and the corresponding ones in the literature. Based on the results of the study, it can be conformed that the proposed numerical method can be applied to stress concentration and crack problems more easily with relatively coarse and simple model than other computational methods and can directly determine the coefficients, not only stress intensity factors (SIFs) but also T -stress and higher order coefficients terms of stress fields near a crack-tip.

References

- Chidgze, S.R. and Deeks, A.J. (2005), "Determination of coefficients of crack-tip asymptotic fields using scaled boundary finite element method", *Eng. Fract. Mech.*, **72**, 2019-2036.
- Deeks, A.J. (2002), "Calculation of stress-intensity factors using the scaled boundary finite-element method", *Proc. Int. Conf. Struct. Integrity and Fracture*, Perth, 3-8.
- Deeks, A.J. and Wolf, J.P. (2002a), "An h -hierarchical adaptive procedure for the scaled boundary finite-element method", *Int. J. Numer. Meth. Eng.*, **54**, 585-605.
- Deeks, A.J. and Wolf, J.P. (2002b), "Stress recovery and error estimation for the scaled boundary finite-element method." *Int. J. Numer. Meth. Eng.*, **54**(4), 557-583.
- Deeks, A.J. and Wolf, J.P. (2002c), "A virtual work derivation of the scaled boundary finite element method for elastostatics", *Comput. Mech.*, **28**, 489-509.
- Du, Z.Z. and Hancock, J.W. (1991), "The effect of non-singular stresses on crack-tip constraint", *J. Mechanics and Physics of Solids*, **39**, 555-567.
- Dyskin, A.V. (1997), "Crack growth criteria incorporating non-singular stresses: Size effects in apparent fracture toughness", *Int. J. Fracture*, **83**, 191-206.
- Jeon, I. and Im, S. (2001), "The role of higher order eigenfields in elastic-plastic cracks", *J. Mechanics and Physics of Solids*, **49**, 2789-2818.
- Karihaloo, B.L. and Xiao, Q.Z. (2001), "Accurate determination of the coefficients of elastic crack tip asymptotic field by a hybrid crack elements with p -adaptivity", *Eng. Fract. Mech.*, **68**, 1609-1630.
- Larsson, S.G. and Carlsson, A.J. (1973), "Influence of non-singular stress terms and specimen geometry on the small-scale yielding at crack-tip in elasto-plastic material", *J. Mechanics and Physics of Solids*, **21**, 263-277.
- Oh, H.S., and Babuska, I. (1992), "The p -version of the finite element method for the elliptic boundary value problems with interfaces", *Comput. Meth. Appl. Mech. Eng.*, **97**, 211-231.
- Rahaulkumar, P., Saigal, S., and Yunus, S. (1997), "Singular p -version finite elements for stress intensity factor computations", *Int. J. Numer. Meth. Eng.*, **40**, 1091-1114.
- Song, C. (2004), "A super-element for crack analysis in the time domain", *Int. J. Numer. Meth. Eng.*, **61**, 1332-1357.
- Song, C. (2005), "Evaluation of power-logarithmic singularities, T -stresses and higher order terms of in-plane singular stress fields at cracks and multi-material corners", *Eng. Fract. Mech.*, **72**, 1498-1530.
- Song, C. and Wolf, J.P. (2002), "Semi-analytical representation of stress singularity as occurring in cracks in anisotropic multi-materials with the scaled boundary finite-element method", *Comput. Struct.*, **80**, 183-197.
- Tan, C.L. and Wang, X. (2003), "The use of quarter-point crack-tip elements for T -stress determination in boundary element method analysis", *Eng. Fract. Mech.*, **70**, 2247-2252.

- Wang, X. (2002), "Determination of weight function for elastic T -stress from reference T -stress solution", *Fatigue & Fracture of Engineering Materials and Structures*, **25**, 965-973.
- Williams, M.L. (1957), "On the stress distribution at the base of a stationary crack", *J. Appl. Mech.*, ASME, **24**, 109-114.
- Wolf, J.P. (2003), *The Scaled Boundary Finite Element Method*, John Wiley & Sons Ltd, England.
- Xiao, Q.Z., Karihaloo, B.L. and Liu, X.Y. (2004), "Direct determination of SIF and higher order terms of mixed mode cracks by a hybrid crack element", *Int. J. of Fracture*, **125**, 207-225.
- Yan, X. (2004), "A numerical analysis of cracks emanating from a square hole in a rectangular plate under biaxial loads", *Eng. Fract. Mech.*, **71**, 1615-1623
- Yang, S., Chao, Y.J. and Sutton M.A. (1993), "Higher order asymptotic crack-tip fields in a power-law hardening materials", *Eng. Fract. Mech.*, **45**, 1-20.